Design and modeling of a photonic crystal fiber gas sensor

Yeuk L. Hoo, Wei Jin, Chunzheng Shi, Hoi L. Ho, Dong N. Wang, and Shuang C. Ruan

We report the modeling results of an all-fiber gas detector that uses photonic crystal fiber (PCF). The relative sensitivity of the PCF as a function of the fiber parameters is calculated. Gas-diffusion dynamics that affect the sensor response time is investigated theoretically and experimentally. A practical PCF sensor aiming for high sensitivity gas detection is proposed. © 2003 Optical Society of America

OCIS codes: 060.2370, 290.1990, 330.1880.

1. Introduction

Photonic crystal fiber (PCF) or holey fiber that incorporates air holes within the silica cladding region opens new opportunities for exploiting the interaction of light with gases through the evanescent field in the holes.[1,2] The use of the evanescent field for gas detection was exploited previously by using D-shaped optical fiber.[3] The sensitivity was, however, very low owing to the 0.2% mode power exposed to the sensing region. Monro *et al.*[1] examined the use of a particular PCF for gas detection and theoretically predicted that by choosing appropriately the PCF parameters, high-sensitivity gas detection can be achieved without significantly compromising the mechanical properties of the optical fiber. A proof of concept demonstration of a PCF gas sensor was recently reported by the authors.[2]

In this paper we report the results of our recent modeling, simulation, and experiments on the design of practical PCF gas sensors. We present first in Section 2 our simulation results on the relative sensitivities of two types of PCF, i.e., the nonlinear PCF with a 1.7-μm core from Crystal Fiber[4] and the Lucent Technology PCF (Ref. 5) with a 1.55-μm hole separation (~1.7-μm-diameter core) and a 1.4-μm hole diameter. We then examine the effect of varying the hole's size and separation on the relative sensitivity of the PCF. The sensor response time limited by gas diffusion into the holes as a function sensing fiber length is modeled and reported in Section 3. Experimental investigations on the relative sensitivity and gas-diffusion dynamics into the air-hole column of the Crystal Fiber PCF is reported in Section 4. Based on the findings in Sections 2–4, a gas (acetylene) sensor design based on a periodically windowed PCF is proposed in Section 5. The power budget and performance analysis of the proposed sensor system are also presented in Section 5. A brief summary is in Section 6.

2. Relative Sensitivity of the Gas Sensor of the Photonic Crystal Fiber

We consider here the index-guided PCF (Refs. 4 and 5) where most of the guided light power is confined within the solid-core region with a fraction (evanescent field) of power extended into the holey region. The evanescent field in the air holes is absorbed by the gas species, and the gas concentration can be obtained from the intensity attenuation through the Beer–Lambert law[6]:

$$I(\lambda) = I_0(\lambda)\exp[-r\alpha_m(\lambda)lC]. \quad (1)$$

I and I_0 are, respectively, the output light intensities with and without the presence of gas being detected, $\alpha_m(\lambda)$ is the absorption coefficient of the gas being measured and is a function of wavelength, l is the length of the PCF used for gas detection (interaction length), C is the gas concentration and r is a relative sensitivity coefficient defined as[6]

$$r = (n_r/n_e)f, \quad (2)$$

Y. L. Hoo, W. Jin, C. Shi, H. L. Ho, and D. N. Wang are with the Department of Electrical Engineering, The Hong Kong Polytechnic University, Hung Hom, Kowloon, Hong Kong, China. S. C. Ruan is with the Faculty of Engineering and Technology, Shenzhen University, Guang Dong, China.

Received 19 July 2002; revised manuscript received 10 December 2002.

0003-6935/03/183509-07$15.00/0

where n_r is the index of the gas species and is approximately equal to 1, n_e is the effective index of the guided mode, and f is the fraction of the total power located in the holes. For a particular fiber mode f can be calculated by integrating the optical power inside the air holes and dividing it by the total power carried by that mode and expressed as

$$f = \int_{\text{holes}} (E_x H_y - E_y H_x)\mathrm{d}x\mathrm{d}y \Big/ \int_{\text{total}} (E_x H_y - E_y H_x)\mathrm{d}x\mathrm{d}y, \quad (3)$$

where E_x, E_y and H_x, H_y are, respectively, the transverse electric and magnetic fields of the mode. The effective index n_e and the mode-field pattern (E_x, E_y and H_x, H_y) can be calculated by solving Maxwell's equations by using a numerical technique (the finite-element method).[7,8]

Two types of PCF, i.e., the Crystal Fiber PCF and the Lucent Technology PCF, were examined. Both PCFs have an ~1.7-μm-diameter silica core surrounded by an array of air holes. During numerical calculation we considered only the two innermost rings and a quarter of the cross section of the fibers as shown in Figs. 1 and 2. The basis for doing so is that, for both types of fiber, most of the guided power, especially for the fundamental mode we are interested in here, is distributed within the central silica core and the innermost ring, and the light power in the outer rings is negligible. The field distributions in the other three quarters can be obtained by using the symmetric property of the fiber. The relative sensitivity of the Crystal Fiber PCF as a function of wavelength is shown in Fig. 3. At wavelengths of 1.53 and 1.65 μm, corresponding to absorption lines of acetylene (C_2H_2) and methane (CH_4) gases, the relative sensitivities are, respectively, 12.6% and 14.9% of that of an open path cell per equal length. This sensitivity is more than 50 times that of the D-shaped optical fiber.[3] The relative sensitivity of Lucent's PCF with 1.4-μm-diameter d air holes and 1.55-μm holes of separation Λ as a function of wavelength is shown in Fig. 4. At 1.53 and 1.65 μm the relative sensitivities are, respectively, 3.8% and 4.7% of that of an open path cell per equal length. We also calculated the relative sensitivity of a modified fiber with the same structure as the Lucent fiber but with varying hole diameter and separation. Figure 4 shows the results for Λ = 1.33 μm and d/Λ varying from 0.69 to 0.93. The relative sensitivity for Λ = 1.33 μm and d = 1.24 μm (d/Λ = 0.93) is 6.2% at a wavelength of 1.53 μm and 7.7% at 1.65 μm.

Although it is difficult to establish an analytical relationship between the relative sensitivity and fiber parameters d, Λ, and wavelength λ from the simulation results, we may conclude that the sensitivity increases with λ and d/Λ but decreases with structural size d or Λ (for the same d/Λ). It can be seen from Fig. 4 that, for the same value of d/Λ = 0.9 and

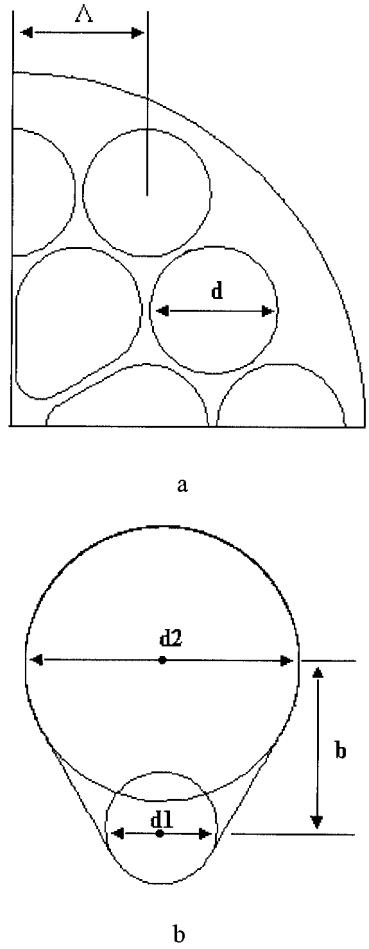

Fig. 1. a, Quarter of the cross section showing the two innermost rings of Crystal Fiber's PCF. The diameter of the central silica region is 1.7 μm. Λ = 3.24 μm and d = 3 μm. b, Shape of the holes in the innermost ring: $d1$ = 1.22 μm, $d2$ = 3 μm, b = 1.79 μm.

at a wavelength of 1.53 μm, the relative sensitivity increases from 3.8% to 5.8% as the hole separation decreases from 1.55 μm (the Lucent fiber) to 1.33 μm. One simple method for designing the relative sensitivity of the PCF is to use the scaling properties of the Maxwell equations in combination with the simula-

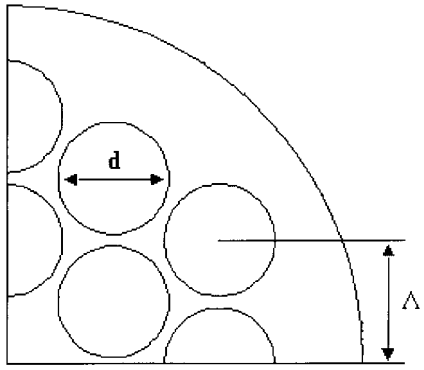

Fig. 2. Quarter of the cross section of Lucent's PCF: Λ = 1.55 μm and d = 1.4 μm.

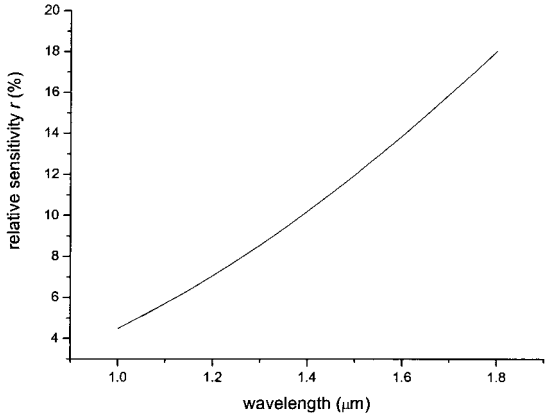

Fig. 3. Relative sensitivity of Crystal Fiber's PCF as a function of wavelength.

tion results in Fig. 4. For example, if we wish to design a PCF with 3.78% relative sensitivity at a wavelength of 1.65 μm (one of the methane absorption wavelengths), we need only to increase the size (d, Λ) of the PCF with 3.78% relative sensitivity (Fig. 4) by a factor S that equals the new working wavelength divided by the old working wavelength, i.e., $S = 1.65/1.53 = 1.0784$. The new fiber parameter should then be $\Lambda = 1.67$ μm and $d = 1.5$ μm. With this method the results at one length scale can be used to deduce the design parameters at all other length scales.

3. Response Time of the Sensor of the Photonic Crystal Fibers

One concern in using PCF as evanescent field sensors may be the limited response time due to the time required for gas to diffuse into the holes. To study this effect, we take acetylene gas as an example and study its diffusion into the holes of a PCF of length l with two ends open (Fig. 5). We assume that the PCF is placed initially in air, and the air-hole columns of PCF were entirely filled with air. At time $t = 0$ the surrounding air is suddenly replaced by acetylene gas with concentration C_0. This sudden change will start a transient mass transportation (transient diffusion) between the air and acetylene. The air will diffuse out from the two ends of the PCF column, and the acetylene will diffuse into the column. At time t the distribution of acetylene concentration along the length of the air hole columns may be written as[9]

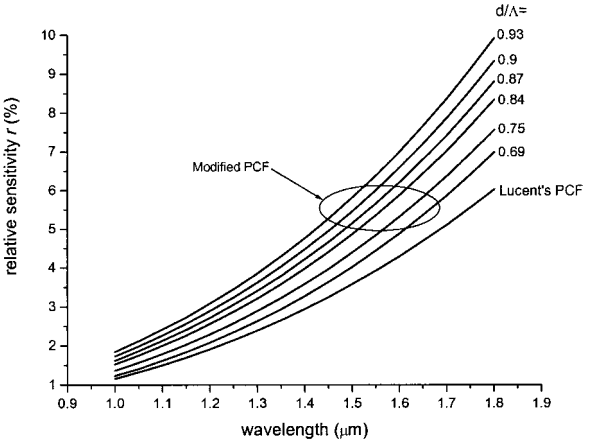

Fig. 4. Relative sensitivities of Lucent's and the modified Lucent's PCFs as functions of wavelength: Lucent's PCF, $\Lambda = 1.55$ μm, $d = 1.4$ μm, $d/\Lambda = 0.9$; modified PCF, $\Lambda = 1.33$ μm and the varying hole diameter corresponding to d/Λ from 0.69 to 0.93.

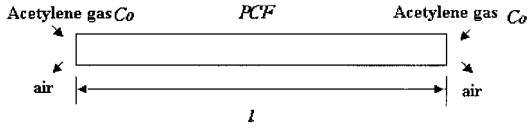

Fig. 5. Gas diffusion into the holes of the PCF of length l.

$$C(x, t) = C_0\left(1 - (4/\pi)\sum_{j=1,3,5}^{\infty}(1/j) \times \{\sin(j\pi x/l)\exp[-(j\pi/l)^2 Dt]\}\right), \quad (4)$$

where D is the binary diffusion coefficient between the air and acetylene and can be found in the reference book[10] and x is the spatial coordinate along the longitudinal direction of the PCF. The acetylene concentrations at the two ends of the PCF are assumed to be C_0 in the whole diffusion process $(t > 0)$. The diffusion is assumed to take place at room temperature and atmospheric pressure.

The average gas concentration over the entire sensing length l as a function of time

$$C_A(t) = \frac{1}{l}\int_0^l C(x, t)\mathrm{d}x \quad (5)$$

may be measured from the intensity attenuation caused by gas absorption through the Beer–Lambert law as given in Eq. (1) but with C replaced by $C_A(t)$.

By substituting Eq. (4) into Eq. (5), we obtain

$$C_A = C_0\left\{1 - (8/\pi^2)\sum_{j=1,3,5}^{\infty}(1/j^2)\exp[-(j\pi/l)^2 Dt]\right\}. \quad (6)$$

It can be seen from Eq. (6) that the average gas concentration in the hole columns depends on interaction length l. For a short interaction length, i.e., $l \to 0$, $C_A(t)$ quickly approaches C_0. When l is 1 m the time for $^{12}C_2H_2$ gas from $C_A(t)$ to reach 90% C_0 is 200 min. Because the size of the holes in the PCF is small, the wall effect between the molecules and the wall of the hole column may also need to be taken into account. The Knudsen number $(K_n = m/d)$ is usually used to represent the wall effect of a capillary diffusion system,[11] where m is the mean free path of the gas molecules and d is the diameter of the capillary tube (the hole diameter here). If the Knudsen number is small, the diffusion has the same charac-

teristics as in the continuum state. If the Knudsen number is larger than one, the diffusion will be dominated by the wall effect. We now study the diffusion of acetylene gas into the holes of Crystal Fiber's PCF. Because guided light power is mainly limited to within the innermost ring of holes, we need to consider only the gas diffusion into these holes. Because the shape of these holes is irregular, we may use the smallest diameter d as shown in Fig. 1a to estimate the maximum Knudsen number. The Knudsen numbers of acetylene and air in the column of these holes were found to be relativity small (less than 0.054), so that the diffusion process is close to the continuum state, plus a small correction factor. Actually the wall effect also induces the viscous flux in the system and superimposes on the diffusive flux, but the effect is so small and complicated that we are concerned only with the diffusive flux in the simulation. In most systems, air can be assumed to be an independent species. The corrected binary diffusion coefficient $D_{AB}{}^{C}$ of B (acetylene) in A (air) may be shown as[12]

$$D_{AB}{}^{C} = D_{AB}D_{BB}{}^{K}/(D_{AB} + D_{AB}{}^{K}), \tag{7}$$

where D_{AB} is the diffusion coefficient of air and acetylene in the continuum state, $D_{AB}{}^{K}$ is the combined Knudsen diffusion coefficient and can be written as[12]

$$D_{AB}{}^{K} \equiv D_{AA}{}^{K}X_B + D_{BB}{}^{K}X_A, \tag{8}$$

where X_A and X_B are the molar fractions of species A and B and $D_{AA}{}^{K}$ and $D_{BB}{}^{K}$ are the Knudsen diffusion coefficients of species A and B, which may be written as[12]

$$D_{\phi\phi}{}^{K} = (1/3)dV_{\phi}, \tag{9}$$

where V_{ϕ} is the average molecular speed of species ϕ (ϕ = A or B). From Eq. (8) it can be seen that $D_{AB}{}^{K}$ and thus $D_{AB}{}^{C}$ are different at every point along the PCF and also changes with time in the whole diffusion process. This made it difficult to compute the exact time taken for the diffusion process. However, we may estimate the diffusion time under the worst plan by replacing $D_{AB}{}^{K}$ in Eq. (7) with $D_{BB}{}^{K}$. The value of $D_{BB}{}^{K}$ (acetylene, 2.069 $cm^2\ s^{-1}$) is larger than $D_{AA}{}^{K}$ (air, 1.966 $cm^2\ s^{-1}$), and thus the estimated value of $D_{AB}{}^{C}$ from Eq. (7) will be the minimum possible value of $D_{AB}{}^{C}$. The diffusion time estimated with Eqs. (6) and (7) will then be the longest possible. The diffusion coefficient of acetylene in air in the continuum state is 0.17774 $cm^2\ s^{-1}$,[10] and the corrected diffusion coefficient in the innermost air-hole column (Fig. 1b) is 0.163 $cm^2\ s^{-1}$ (8.3% decreasing). Figure 6 shows the normalized average concentration inside the hole column against the time for a range of fiber lengths l at room temperature (20 °C) and atmospheric pressure.

If we take the time for $C_A(t)$ to reach 90% C_0 as the response time of the fiber, the response times for 3-, 5-, and 7-cm lengths of fiber with both ends open for diffusion are found to be 11.7, 32.5, and 62.7 s, respectively.

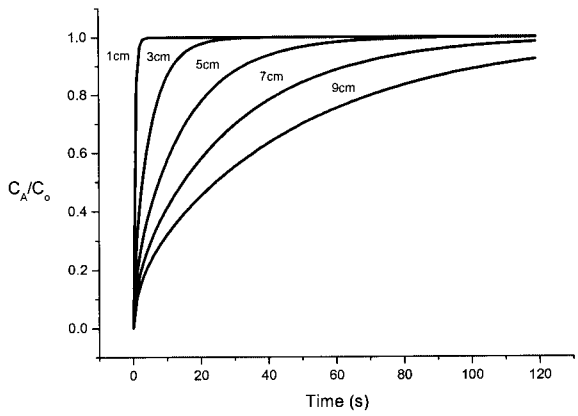

Fig. 6. Normalized average concentration inside the hole's column against the time for a range of fiber lengths l. Diffusion is assumed to be from both ends and with the wall effect considered.

4. Experiments and Results

Experiments were conducted to investigate the relative sensitivity and the diffusion dynamics of Crystal Fiber's PCF for acetylene measurement. The experimental setup is shown in Fig. 7. Light from an Er-doped amplified spontaneous emission source passes through a tunable optic filter (TOF) of ~0.02-nm bandwidth before coupling into the PCF. The single-mode pigtail of the TOF was butt coupled to the PCF with an ~50-μm gap between the two fiber ends to allow for gas diffusion into the holes of the PCF. The butt-coupled joint was put inside a gas chamber with a volume of 6 cm × 6 cm × 6 cm. The other end of the PCF was spliced to a single-mode fiber connected to a photodetector. The spliced end was effectively sealed and the experimental system can be regarded as a diffusion system with a single open end.

Before the start of the experiments the chamber was filled with air. Acetylene gas with a concentration approaching C_0 = 100% was blown into the chamber along a direction orthogonal to the PCF with a blow rate of 100 cm^3/s. The cross-sectional area of the outlet valve is ~2 cm^2 and is ~4 times bigger than that of inlet in order to prevent additional pressure that may affect the diffusion process when the C_2H_2 was loaded into the chamber. The chamber was then sealed after 30 s of loading of acetylene. During the experiments the TOF was repeatedly scanned around the absorption line of acetylene ($^{12}C_2H_2$) at 1531.53 nm with a repetition rate of ~0.1 Hz. Dur-

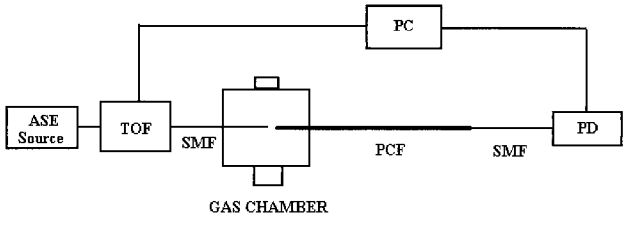

Fig. 7. Experimental setup: SMF, single-mode fiber; PD, photodetector.

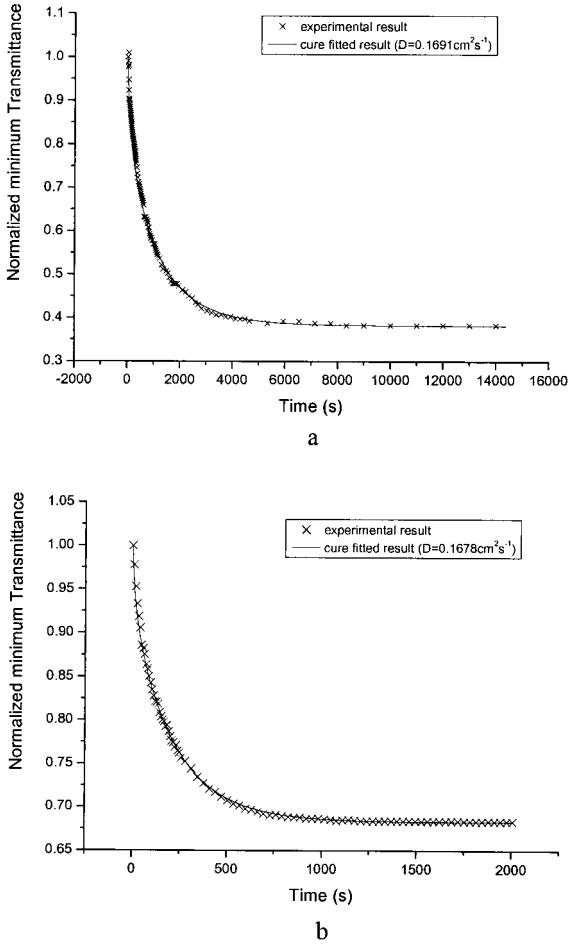

Fig. 8. Measured normalized minimum transmittance as a function of time: a, 25-cm-long PCF; b, 10-cm-long PCF.

ing each scan the minimum transmittance corresponding to the peak absorption at 1531.53 nm was recorded with a PC that is also used to control the TOF. The room temperature was at ~293 K. Figures 8a and 8b show the measured normalized minimum transmittances as functions of time for a 25- and 10-cm-long Crystal Fiber PCF, respectively. The transmittances reach steady states at ~8000 and 2000 s for the 25- and the 10-cm PCFs, respectively.

For comparison we modeled the variation of the (minimum) transmittance as a function of time. By using Eqs. (1) and (6), we may express light intensity at the photodetector as

$$I = I_0 \exp\left(-r\alpha_m l\left\{1 - (8/\pi^2)\sum_{j=1,3,5}^{\infty} \times (1/j^2)\exp[-(j\pi/2l)^2 Dt]\right\}\right). \quad (10)$$

In deriving Eq. (10), we assume that the concentration of acetylene in the chamber was constant (C_0 = 100% acetylene) over the whole measurement period. This is justified because the volume of the chamber is 1.96×10^6 times bigger than that of the air-hole columns of the fiber, and consumption of acetylene

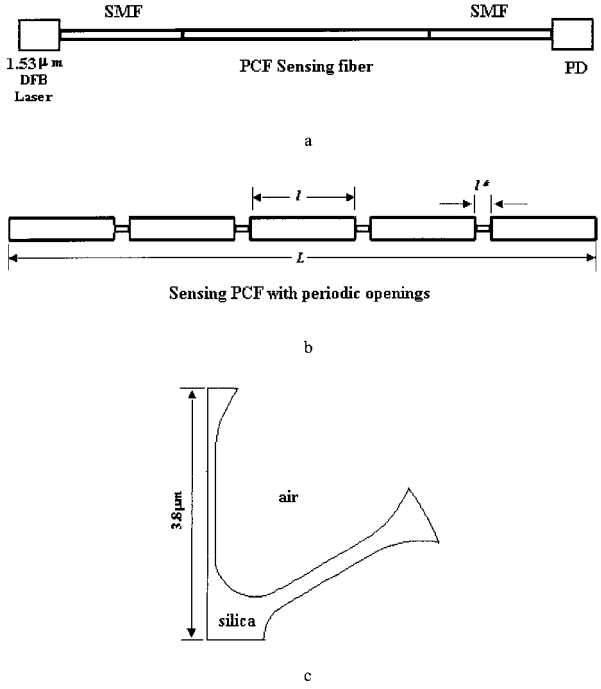

Fig. 9. a, PCF acetylene gas-sensing system: SMF, single-mode fiber; PD, photodetector; b, PCF with periodic openings; c, Quarter of the cross section of the Crystal Fiber's PCF with opening.

within the chamber over the measurement period is negligible. We also replaced l in Eq. (6) with $2l$ in Eq. (10) because the experimental system uses a PCF with a single open end and is equivalent to a system of twice the length of the PCF of the two-end open system. The parameters in Eq. (10) can be obtained from various measurements. The absorption coefficient α_m was measured with a direct absorption cell to be 0.2806 cm^{-1}. The relativity sensitivity r was estimated by using the steady-state [$t \to \infty$ in Eq. (10)] value of the normalized minimum transmittance as shown in Fig. 9. The steady values for the 25- and 10-cm PCFs are, respectively, 0.3827 and 0.6835, giving relative sensitivities of 13.75% and 13.59%. These values are close to the simulation results of 12.6% for the fundamental mode (Fig. 3). With r = 13.7% and α_m = 0.2806 we fitted the measurement data in Fig. 8 to Eq. (10) and found that the diffusion coefficients for the 25- and 10-cm PCFs are, respectively, D = 0.169 $cm^2\ s^{-1}$ and D = 0.168 $cm^2\ s^{-1}$.

These values are again close to the corrected diffusion coefficient (0.163 $cm^2\ s^{-1}$) obtained in Section 3. The agreements in the theoretical calculated and the experimental measured (fitted) values of D and r confirmed that the modeling techniques used for predicting the relativity sensitivity and the diffusion dynamics of the PCFs are accurate. The same techniques may be used to evaluate the performance of sensors made from PCFs with other geometries. The small discrepancies between the theory and the experiments may be

due to the real fiber parameters being slightly different from that used in the modeling.

5. Sensor Design, Power Budget Analysis, and Performance Evaluation

From the analysis in Section 4 we conclude that the response time of PCF is limited by the time taken for acetylene gas to diffuse into the holes. For a gas-sensing application that requires a response time of ~1 min the length of the sensing PCF should be limited to less than 7 cm. The sensitivity of the sensor is then limited because of the short sensing fiber length allowed. To achieve a higher sensitivity with a reasonable response time, we propose introducing periodic openings along the sensing fiber. This design allows for a long sensing fiber to be used to improve the sensitivity without comprising response time. Figure 9a shows an example of a sensor design based on Crystal Fiber's ~1.7-μm-diameter silica core PCF where the sensing PCF with periodic openings is connected to single-mode transmission fibers at the two ends. A 1.53-μm distributed feedback laser is used as the source and an InGaAs photodetector as the receiver. The sensing PCF with periodically open windows is shown in Fig. 9b and the cross section of the PCF with an opening is shown in Fig. 9c.

A. Loss Introduced from the Opening

The openings in the PCF modify the waveguide structure and thus change the transversal field distribution in the fiber cross section. For the ~1.7-μm-diameter silica core PCF from Crystal Fiber with openings as shown in Fig. 9c, because most of the light power is concentrated in the core and the regions within the inner most rings of holes that are close to the core, the variation in the field distribution due to the introduction of an opening is expected to be small. The power loss occurs at the transition between the PCFs with and without an opening because the mismatch of the modal field pattern may be calculated with[13]

$$\alpha = \left\{ [2\sqrt{n_e}\ \sqrt{n_e^c}/(n_e + n_e^c)] \left[\int E \cdot E_c \, \mathrm{d}a \Big/ \left(\int E \cdot E \, \mathrm{d}a \right)^{1/2} \left(\int E_c \cdot E_c \, \mathrm{d}a \right)^{1/2} \right] \right\}^2, \quad (11)$$

where n_e, n_e^c and E, E_c are, respectively, the effective indexes and the transverse electric-field distributions of the PCF with and without an opening. The $2\sqrt{n_e}\ \sqrt{n_e^c}/(n_e + n_e^c)$ in Eq. (11) is the Fresnel coefficient, and the second term is the overlap integral between the fundamental modes of the respective PCF sections. In our simulation we found the fundamental modes of both the cut and the original PCF at the 1531.5-μm wavelength and then substituted the mode field into the Eq. (11) to obtain the power coupled fraction. Results show that the difference in the effective indexes with and without an opening is very small, and the first term is approximately equal to 1. The calculated power loss is $\alpha = 0.0014$ dB.

B. Lengths of the Open Sections

The lengths of the opened sections (l^* as shown in Fig. 9b) should be long enough to ensure that time required for (acetylene) gas diffusion into the holes is not dominated by the wall effect of the open sections. To achieve this, the Knudsen number ($K_n = m/l^*$) should be much smaller than 1. Assuming that $K_n \leq 0.01$, the length of the open section should be longer than 6.5 μm. Because the depth of the open fiber section is less than the radius of the original PCF (~65 μm), the time required for the acetylene to diffuse into the open air holes is estimated to be less than 0.001 s. This value is significantly smaller than the time necessary for diffusion through the unopen air-hole columns and can therefore be neglected in the evaluation of the response time.

As mentioned in this subsection the variation in the mode-field distribution due to the opening is small. As a matter of fact, the mode field in the open section is slightly mode confined within the core region because of the relatively low refractive index of the air compared with that of the silica. Because the open section is so short, the bending effect can then be avoided. The loss coefficient in the open section is then expected to be similar to that of the unopen fiber sections.[14] The loss due to the opening is thus mainly due to that occurring at the transition between the open and unopened PCFs and can then be calculated by Eq. (11).

C. Power Budget and Performance Analysis

Considering as an example the sensor system shown in Fig. 9 with a required response time of ~1 min, the fiber length between the two open windows can be chosen as $l = \sim 7$ cm. For a total fiber-sensing length of L centimeters, the number of openings required will be $L/7$ and loss due to the openings will be $2\alpha L/7$. The source power P_s, fiber length L, maximum gas concentration $C_{\max}$, and the minimum detectable power of photoreceiver P_D should satisfy

$$P_s - (2\alpha L/7) - \alpha_f L - r\alpha_m C_{\max} L \geq P_D, \quad (12)$$

where α_m is the absorption coefficient of gas at the operating wavelength and equals 1.218 dB cm^{-1} for acetylene detection at 1.5315 μm, r is the relative sensitivity of the PCF and equals 13.72% for the Crystal Fiber PCF working at 1.5315 μm, and α_f represents the loss of the PCF and is ~0.1 dB/m for the Crystal Fiber PCF.[5] For typical values of $P_s = 5$ mW (7 dBm), $P_D = 10$ nW (−50 dBm), $\alpha = 0.0014$ dB, and $C_{\max} = 5\%$, the maximum sensing length can be calculated as $L = 4.87$ m. This is equivalent to an open-path gas cell with an equivalent length of $4.87 \times 13.72\% = 0.668$ m! Consider that the detection resolution of 3.75 parts per million for an equivalent of 1 m (ppm m) of acetylene has been achieved with wavelength modulation spectroscopy and digital signal processing.[15,16] We expect that, with the same

optoelectronic processing circuits, the detection resolution with the 4.87-m PCF to be 3.75 ppm/0.668 = 5.6 ppm.

6. Summary

We have proposed an all-fiber gas sensor based on periodically windowed PCF fiber. Preliminary experiments and simulation show that an acetylene sensor system with a response time of ~1 min and sensitivity of better than 6 ppm can be realized. The PCF sensor can also be used to detect other gases such as methane with a similar expected performance. The response time may be tailored with a certain range by selecting the distance between the two windowed sections. To realize a practical sensor system, a number of practical issues need to be solved. These include the low-loss connection between the single-mode transmission fibers and the PCF sensing fiber, fabrication of the window openings along the PCF, and packaging of the open section with gas permeable films that allow gas to diffuse in or out but prevent dirt to enter the open sections.

References

1. T. M. Monro, D. J. Richardson, and P. J. Bennett, "Developing holey fibers for evanescent field devices," Electron. Lett. **35,** 1188–1189 (1999).
2. Y. L. Hoo, W. Jin, H. L. Ho, D. N. Wang, and R. S. Windeler, "Evanescent-wave gas sensing using microstructure fiber," Opt. Eng. **41,** 8–9 (2002).
3. G. Stewart, W. Jin, and B. Culshaw, "Prospects for fiber-optic evanescent-field gas sensors using absorption in the near field," Sens. Actuators B **38,** 42–47 (1997).
4. See www.crystalfiber.com.
5. J. K. Ranka, R. S. Windeler, and A. J. Stentz, "Optical properties of high-delta air-silica microstructure optical fibers," Opt. Lett. **25,** 796–798 (2000).
6. G. Stewart, J. Norris, D. F. Clark, and B. Culshaw, "Evanescent-wave chemical sensors—a theoretical evaluation," Int. J. Optoelectron. **6,** 227–238 (1991).
7. S. Seller and M. Zoboli, "Performance comparison of finite-element approaches for electromagnetic waveguides," J. Opt. Soc. Am. A **14,** 1460–1465 (1997).
8. J. Jin, *The Finite Element Method in Electromagnetics*, 2nd ed. (Wiley, New York, 1993), pp. 273–337.
9. J. Crank, *The Mathematics of Diffusion* (Clarendon, Oxford, 1975), pp. 44–68, 160–202.
10. C. L. Yaws, *Handbook of Transport Property Data: Viscosity, Thermal Conductivity, and Diffusion Coefficients of Liquids and Gases* (Gulf Publishing, Houston, Tex., 1995).
11. E. L. Cussler, *Diffusion: Mass Transfer in Fluid Systems* (Cambridge University, New York, 1997), pp. 173–184.
12. R. E. Cunningham and R. J. J. Williams, *Diffusion in Gases and Porous Media* (Plenum, New York, 1980), pp. 145–151, 243–246.
13. K. Gyeong-il and P. In-shik, "Splicing losses between dissimilar optical waveguides," J. Lightwave Technol. **17,** 690–703 (1999).
14. K. S. Chiang, City University of Hong Kong, Hong Kong (personal communication, 2003).
15. B. Culshaw, G. Stewart, F. Dong, C. Tandy, and D. Moodie, "Fiber optic techniques for remote spectroscopic methane detection—from concept to system realization," Sens. Actuators B **51,** 25–37 (1998).
16. H. L. Hoi, W. Jin, and M. S. Demokan, "Sensitive, multipoint gas detection using TDM and wavelength modulation spectroscopy," Electron. Lett. **36,** 1191–1193 (2000).